Hindawi
Journal of Energy
Volume 2020, Article ID 9710189, 9 pages
https://doi.org/10.1155/2020/9710189

*Research Article*

# Development of High Performance Airfoils for Application in Small Wind Turbine Power Generation

**Emmanuel Yeboah Osei**,[1,2] **Richard Opoku**,[1,3] **Albert K. Sunnu**,[1] **and Muyiwa S. Adaramola**[4]

[1]*Department of Mechanical Engineering, Kwame Nkrumah University of Science and Technology, Kumasi, Ghana*
[2]*Department of Mechanical Engineering, Kumasi Technical University, P. O. Box 854, Kumasi, Ghana*
[3]*The Brew-Hammond Energy Center, Kwame Nkrumah University of Science and Technology, Kumasi, Ghana*
[4]*Faculty of Environmental Sciences and Natural Resource Management, Norwegian University of Life Sciences, Ås, Norway*

Correspondence should be addressed to Emmanuel Yeboah Osei; emma.y.osei@gmail.com

Received 21 November 2019; Revised 15 January 2020; Accepted 20 January 2020; Published 7 February 2020

Academic Editor: Aleksander Zidansek



Small wind turbine power generation systems have the potential to meet the electricity demand of the residential sector in developing countries. However, due to their exposure to low Reynolds number (Re) flow conditions and associated problems, specific airfoils are required for the design of their blades. In this research, XFOIL was used to develop and test three high performance airfoils (EYO7-8, EYO8-8, and EYO9-8) for small wind turbine application. The airfoils were subsequently used in conjunction with Blade Element Momentum Theory to develop and test 3-bladed 6 m diameter wind turbine rotors. The aerodynamic performance parameters of the airfoils tested were lift, drag, lift-to-drag ratio, and stall angle. At Re = 300,000, EYO7-8, EYO8-8, and EYO9-8 had maximum lift-to-drag ratios of 134, 131, and 127, respectively, and maximum lift coefficients of 1.77, 1.81, and 1.81, respectively. The stall angles were 12° for EYO7-8, 14° for EYO8-8, and 15° for EYO9-8. Together, the new airfoils compared favourably with other existing low Re airfoils and are suitable for the design of small wind turbine blades. Analysis of the results showed that the performance improvement of the EYO-Series airfoils is as a result of the design optimization that employed an optimal thickness-to-camber ratio ($t/c$) in the range of 0.85–1.50. Preliminary wind turbine rotor analysis also showed that the EYO7-8, EYO8-8, and EYO9-8 rotors had maximum power coefficients of 0.371, 0.366, and 0.358, respectively.

## 1. Introduction

In many developing countries, access to sustainable energy is a challenge despite abundant renewable energy resources. In sub-Saharan Africa for example, it is estimated that over 600 million people do not have access to electricity [1]. Development of renewable energy resources in the region has been very low compared to other developed regions in the world [2, 3]. Fossil-fuel-based power generation systems have been the main technologies for electricity generation [4]. The increasing effect of climate change and greenhouse gas emissions on the environment, as a result of electricity generation from fossil fuels, is driving a paradigm shift to more environmentally friendly and clean energy resources including solar and wind energy [5–10].

Wind energy is a major clean energy resource which has been demonstrated to be able to produce both small-scale and large-scale energy [8, 11–13]. However, small-scale wind energy generation requires the use of small wind turbine blades made of special airfoils with good aerodynamic performance under low wind speed conditions [14–17].

For small wind turbine applications, low wind speeds are generally characterized by airflows with Reynolds numbers (Re) below 500,000. Under this low Re condition, improperly designed blade airfoils encounter deterioration in aerodynamic performance which adversely affects the operating efficiency of the wind turbine [18–21]. As such, airfoils designed for large-scale wind turbines are not necessarily suitable for small-scale wind turbines [19, 20, 22, 23]. The airfoil aerodynamic parameters of interest in low wind

speed airfoils are the lift-to-drag ratio ($L/D$), lift coefficient, stall angle, stall performance, and drag bucket performance [22, 24–27].

Some airfoils have been developed for low wind speed applications. Gigueŕe and Selig developed and tested four airfoils (SG6040, SG6041, SG6042, and SG6043) for low Re small wind turbine applications [28]. The study recorded improvement in airfoil performance with increasing Re. At Re = 500,000, SG6040, SG6041, SG6042, and SG6043 airfoils had maximum $L/D$ performances of 87, 84, 106, and 125, respectively.

Giguere and Selig studied fifteen airfoils for aerodynamic performance under low Re conditions [29]. The study recorded improvement in aerodynamic performance with increasing Re and relatively better performance for the thinner airfoils. At Re = 300,000, the SD7032 airfoil had the highest maximum $L/D$ of 83, while the S823 airfoil had the lowest value of 63.

Singh et al. developed the AF300 low Re airfoil by geometrically modifying other airfoils using XFOIL and tested it numerically at Re between 38,000 and 205,000 [16]. The aerodynamic performance of the airfoil improved with increase in Re. At Re = 100,000, the AF300 airfoil had maximum $L/D$ of 54 and stall angle of 14°. The study concluded that AF300 is a good airfoil for the design of small wind turbine blades.

Selig and McGranahan studied the aerodynamic performance characteristics of E387, FX63-137, S822, S834, SD2030, and SH3055 airfoils under low Re conditions between 100,000 and 500,000 [15]. At Re of 100,000, SD2030 had the highest maximum $L/D$ of 53 and a stall angle of 12°. However, at Re of 500,000, FX63-137 had the highest maximum $L/D$ of 108 and a stall angle of 12°.

Henriques et al. designed and tested the "T.Urban 10/193" airfoil in XFOIL for application in small horizontal axis wind turbines for urban environment [30]. At Re = 60,000, the maximum $L/D$ and stall angle were 18 and 8°, respectively. However, at Re = 500,000, the maximum $L/D$ and stall angle increased to 95 and 12°, respectively. The "T.Urban 10/193" airfoil was concluded to be a good airfoil for small wind turbine application.

From available literature, a number of studies have been conducted on airfoils for low Re applications in small wind turbines. However, there is no reported study on the aerodynamic performance parameters of airfoils based on thickness-to-camber ratio ($t/c$). In this work, three new airfoils are developed based on a range of optimal airfoil $t/c$ and their aerodynamic performance characteristics are determined for low wind speed and low Re applications. These airfoils, which have high $L/D$, were subsequently used to develop 3-bladed wind turbine rotors, and their power coefficients were determined based on Blade Element Momentum Theory (BEMT). The methodology used in this study is presented in Section 2.

## 2. Methodology

*2.1. Design of the Airfoils and Rotor.* In this study, XFOIL version 6.99 was used as the tool for the airfoil design optimization and simulations. XFOIL is a popular simulation tool for the general design of airfoils [31]. It has simulation capabilities for the determination of airfoil characteristics such as shape, lift, drag, and stall. XFOIL has been used by several researchers for the design and test of airfoils and has been found to produce results that agree well with wind tunnel results [30, 32, 33].

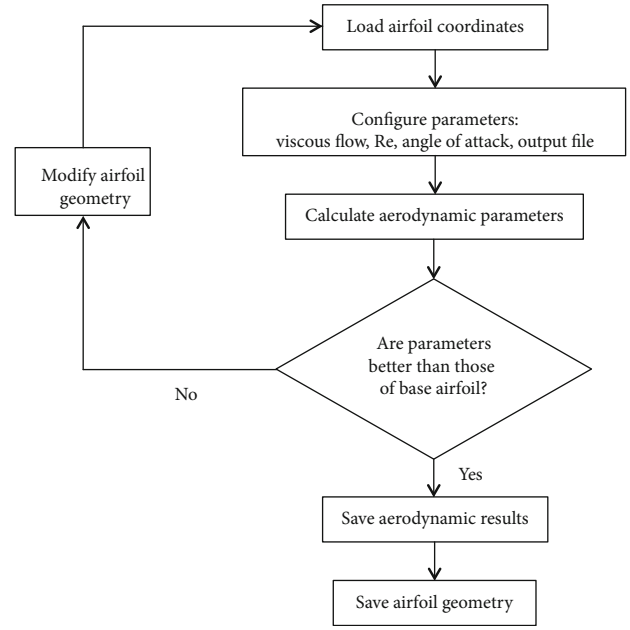


Figure 1: Summary of XFOIL procedure for airfoil design.

To undertake the present study, the SG6043 airfoil reported by [28] was selected as the base airfoil for development of the new airfoils due to its good aerodynamic performance in low Re conditions. The geometry of the base airfoil was redesigned in XFOIL by modifications of the thickness and camber configurations to form new airfoils. At each configuration of $t/c$, the corresponding new airfoil was tested for maximum $L/D$ at Re between 100,000 and 500,000. Afterwards, the optimal zone of $t/c$ for the highest maximum $L/D$ was used to determine the geometrical characteristics of the newly developed airfoils.

The newly developed airfoils were tested for aerodynamic performance parameters (lift, drag, $L/D$, stall, and drag bucket) and compared with the base airfoil at Re = 300,000. This Re was chosen based on average wind speed data of 5 to 6.1 m/s at 12 metres above ground level for Ghana as reported by the Energy Commission [34]. Equation (2) was also used in the determination of the Re based on common small wind turbine rotational speed range of about 400 RPM to 1,500 RPM as reported by [35–38]. The procedure used for the new airfoil designs in XFOIL is summarized in Figure 1.

The airfoil panel nodes used for the computation were 160 coordinate points. The maximum iteration limit used to obtain steady state solution for the XFOIL analysis was 1,000. The flow conditions were configured for viscous flow at Re = 300,000 and for angles of attack ranging from 0° to 20°. Three new airfoils labelled EYO7-8, EYO8-8, and EYO9-8 were subsequently developed, and the performance

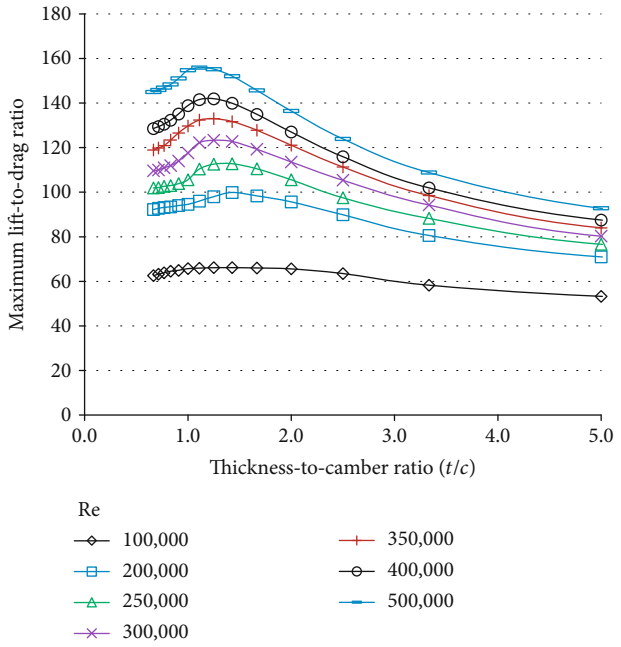


Figure 2: Maximum lift-to-drag ratio at different thickness-to-camber ratios.

parameters are presented in Section 3. BEMT was applied to the three new airfoils to develop 3-bladed 6-metre-diameter wind turbine rotors, and preliminary assessments of their power coefficients were evaluated. The power coefficient data was used to estimate the power generation of each wind turbine rotor based on typical average wind speed conditions in Ghana.

*2.2. Mathematical Framework.* The Re for the airflow over the airfoil is expressed mathematically in Equation (1) [39]. For a typical airfoil in a wind turbine blade section, the relationship between the free stream airflow speed and the relative airflow speed at the airfoil is expressed in Equation (2) [29]. The airfoil lift and drag forces are expressed in Equations (3) and (4), respectively [40]. The lift-to-drag ratio is also expressed in Equation (5).

$$\mathrm{Re} = \frac{\rho U_{\mathrm{rel}} c}{\mu} = \frac{U_{\mathrm{rel}} c}{\nu}, \tag{1}$$

$$U_{\mathrm{rel}} = \sqrt{[U(1-a)]^2 + [\Omega r]^2}, \tag{2}$$

$$L = C_l \frac{1}{2} \rho U^2 cl, \tag{3}$$

$$D = C_d \frac{1}{2} \rho U^2 cl, \tag{4}$$

$$\frac{L}{D} = \frac{(C_l(1/2)\rho U^2 cl)}{(C_d(1/2)\rho U^2 cl)} = \frac{C_l}{C_d}. \tag{5}$$

*2.3. Blade Element Momentum Theory.* Blade Element Momentum Theory (BEMT) uses airfoil information for the design of wind turbine blades for wind power extraction.

Table 1: Thickness and camber information for airfoils.

| Airfoil | Thickness (% c) | Camber (% c) |
|---|---|---|
| Base airfoil (SG6043) | 10 | 5.5 |
| EYO7-8 | 7 | 8 |
| EYO8-8 | 8 | 8 |
| EYO9-8 | 9 | 8 |

BEMT is used extensively for wind turbine blade design and testing. This has been mainly due to the agreement of the theory with experimental data. Several studies on wind turbine rotor design have demonstrated the robustness of BEMT in wind turbine rotor analysis [33, 35, 41–43]. The BEMT equations used for the rotor development are expressed in Equations (6)–(10) [40]. The power generation ($P$) from the turbine rotor is computed from Equation (11) based on the free airstream properties ($\rho$ and $U$), the projected rotor area ($A$), and the power coefficient $C_p$(Equation (10)) [44].

$$\alpha = \phi - \theta_p, \tag{6}$$

$$\sigma_r = \frac{Bc}{2\pi r}, \tag{7}$$

$$\frac{a}{1-a} = \frac{\sigma_r}{4\sin^2\phi} \times (C_l \cos\phi + C_d \sin\phi), \tag{8}$$

$$\frac{a'}{1-a'} = \frac{\sigma_r}{4\sin\phi\cos\phi} \times (C_l \sin\phi - C_d \cos\phi), \tag{9}$$

$$C_p = \frac{8}{\lambda^2} \int_{\lambda_h}^{\lambda} \lambda_r^3 a'(1-a) \left[1 - \left(\frac{C_d}{C_l}\right) \cot\phi\right] d\lambda_r, \tag{10}$$

$$P = C_p \frac{1}{2} \rho A U^3. \tag{11}$$

*2.4. Airfoil Design Optimization.* In the present study, the airfoil design optimization was based on the lift-to-drag ratio ($L/D$) performance for different airfoil $t/c$. From the preliminary results for the design optimization, Figure 2 shows the variations in maximum $L/D$ with $t/c$ at Re between 100,000 and 500,000.

From Figure 2, the maximum $L/D$ had a dome-shaped relation with $t/c$ at each Re, and the $L/D$ performance generally improved with increase in Re. The highest point of the maximum $L/D$ for each Re occurred in about the same range between $t/c$ of 0.85 and 1.50. However, outside this $t/c$ range, the maximum $L/D$ is observed to decrease. In the design of the airfoils in this study, $t/c$ in the range of 0.85–1.50 was considered in determining the thicknesses and camber of the airfoils.

Based on the preliminary findings presented above, the optimal zones chosen for the development of the new airfoils with improved aerodynamic performances were 7% c, 8% c, and 9% c thicknesses and 8% c camber. These thickness and camber characteristics fall within the $t/c$ range of 0.85–1.50. Three airfoils were developed in this zone and were labelled EYO7-8, EYO8-8, and EYO9-8. The geometrical parameters and profiles of these airfoils are presented in

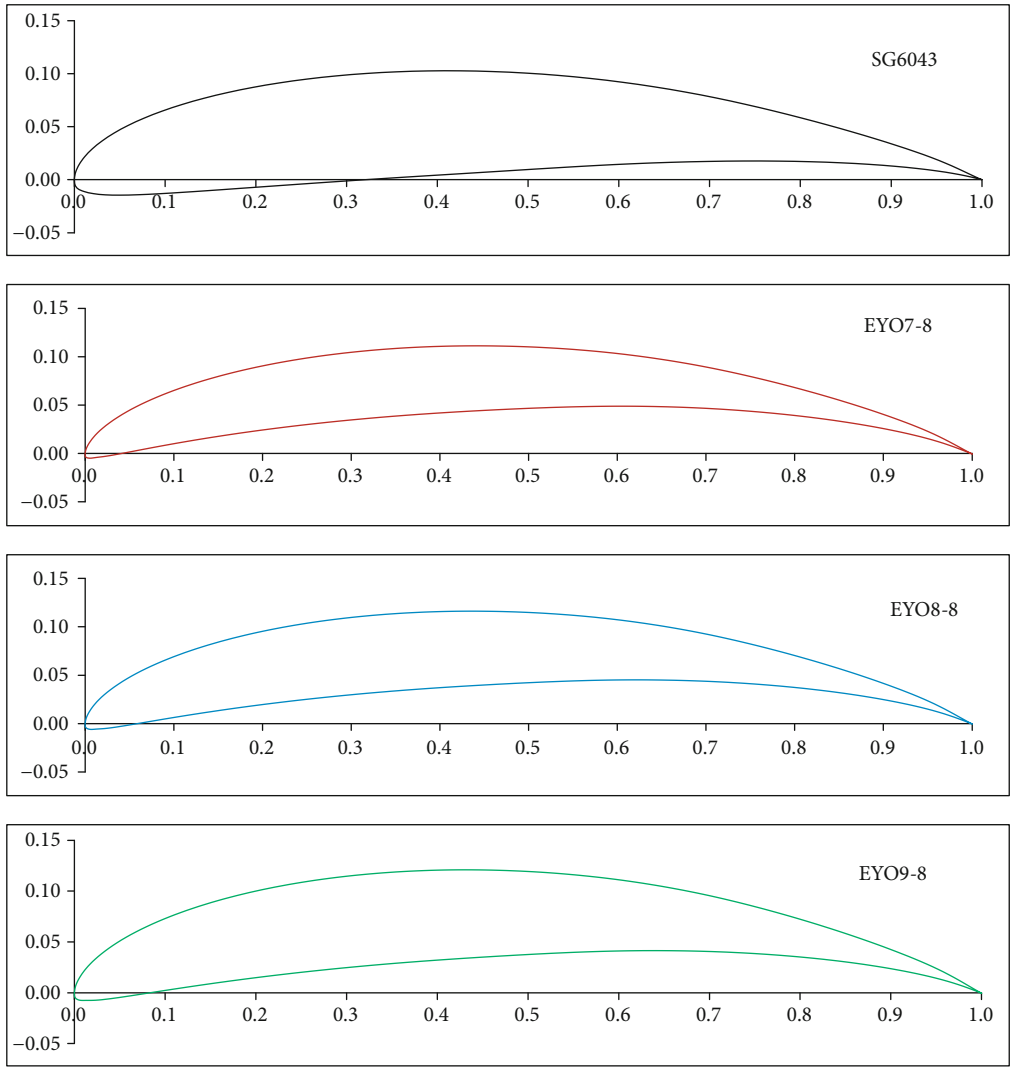


(a) Separate geometries for the airfoils

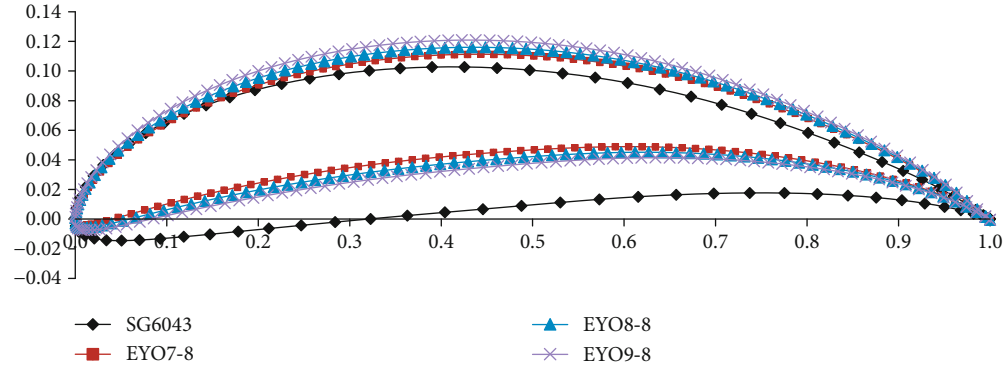


(b) Overlapped geometries for the airfoils

Figure 3: Geometries of base and new EYO-Series airfoils (in dimensionless units).

Table 1 and Figure 3(a), respectively. For the purpose of comparison, the different shapes of the airfoils have been overlapped in Figure 3(b).

From Figure 3, the main difference between the base airfoil and the newly developed EYO-Series airfoils is in the geometrical characteristics of the camber and thickness profiles. The new EYO-Series airfoils have relatively higher cambered and thinner designs compared with the base airfoil. The performance characteristics of the newly designed airfoils as well as the base airfoil were determined at Re of 300,000, as already indicated above, based on average wind speed data of 5 to 6.1 m/s at 12 metres above ground level

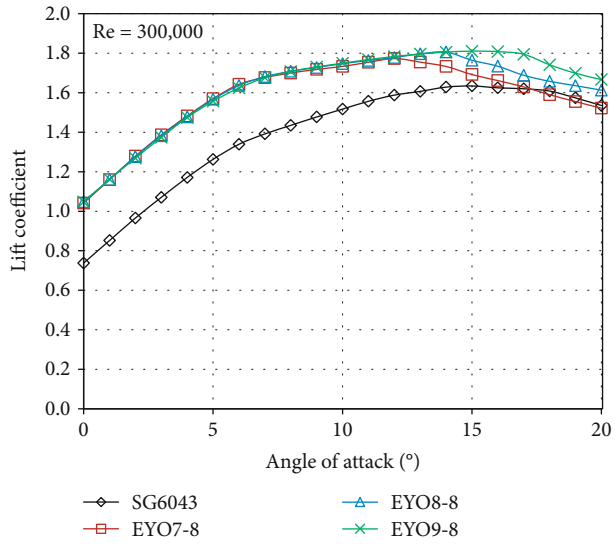


Figure 4: Lift performances of SG6043 and EYO-Series airfoils at Re = 300,000.

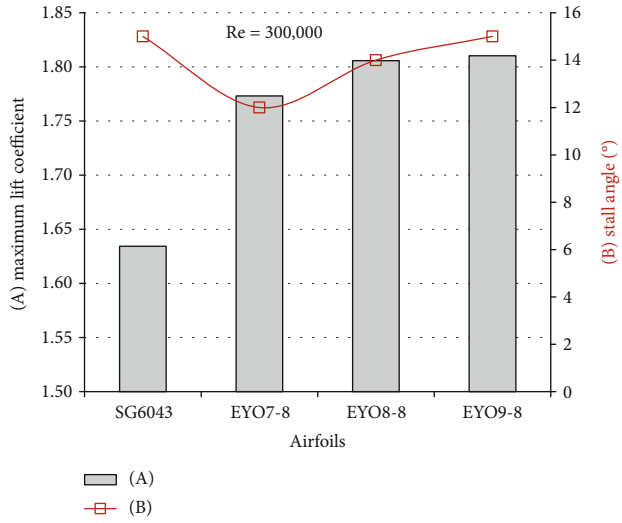


Figure 5: Maximum $C_L$ and stall angles of SG6043 and EYO-Series airfoils at Re = 300,000.

for the study area. The results obtained in this study are presented in Section 3.

## 3. Results and Discussions

*3.1. Comparative Lift Performance of EYO-Series Airfoils and SG6043 Base Airfoil.* The lift coefficient performance curves of the SG6043 and EYO-Series airfoils at Re = 300,000 are presented in Figure 4. The variation of maximum lift coefficient ($C_L$) for the airfoils at the same Re is also presented in Figure 5, in addition to the stall angles.

From Figures 4 and 5, it is observed that the new EYO-Series airfoils have relatively higher lift coefficients than the SG6043 base airfoil. Although the new airfoils had similar lift performance trends for up to 12° angle of attack, the EYO9-8 airfoil had relatively better lift performance for

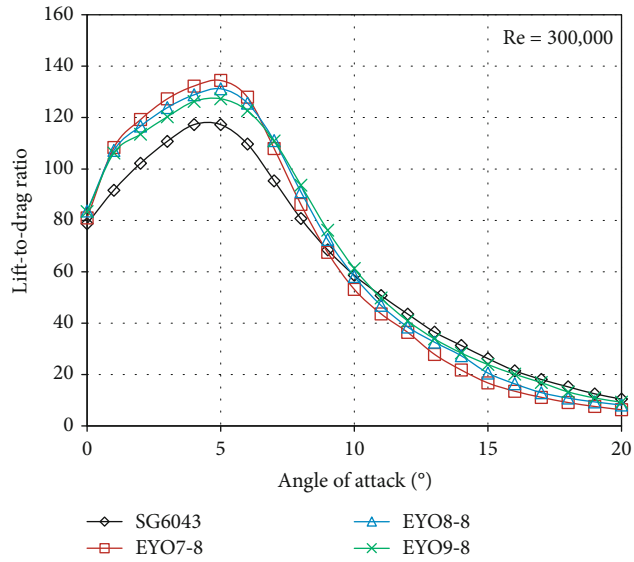


Figure 6: *L*/*D* performances of SG6043 and EYO-Series airfoils at Re = 300,000.

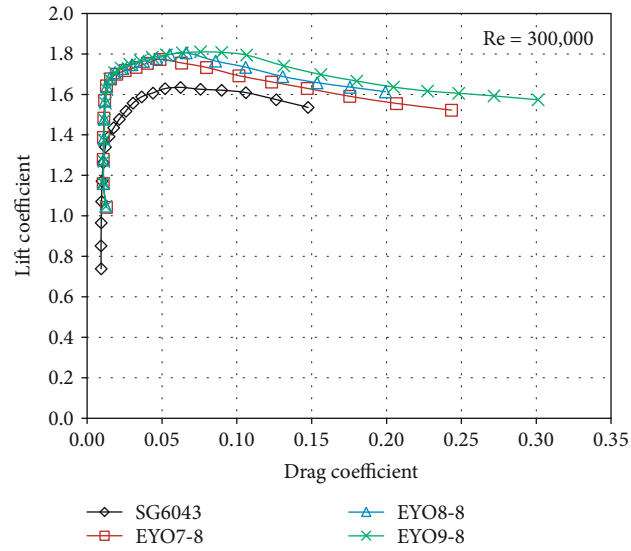


Figure 7: Drag buckets for SG6043 and EYO-Series airfoils at Re = 300,000.

angles of attack beyond 12°. The EYO8-8 and EYO9-8 airfoils had the highest maximum lift coefficient of 1.81 while the SG6043 airfoil had the lowest maximum lift coefficient of 1.63. The EYO7-8 airfoil had maximum lift coefficient of 1.77.

From Figure 5, the SG6043 and EYO9-8 airfoils had the highest stall angle of 15°. The EYO7-8 and EYO8-8 airfoils had stall angles of 12° and 14°, respectively. Again, among the new airfoils and from Figure 4, EYO9-8 had the most gradual stall performance. Gradual stall is desired in airfoil design in order to prevent the sudden loss of lift which could adversely affect wind turbine performance.

*3.2. Comparative Lift-to-Drag Ratio Performances of EYO-Series Airfoils and SG6043 Base Airfoil.* The *L*/*D* performance

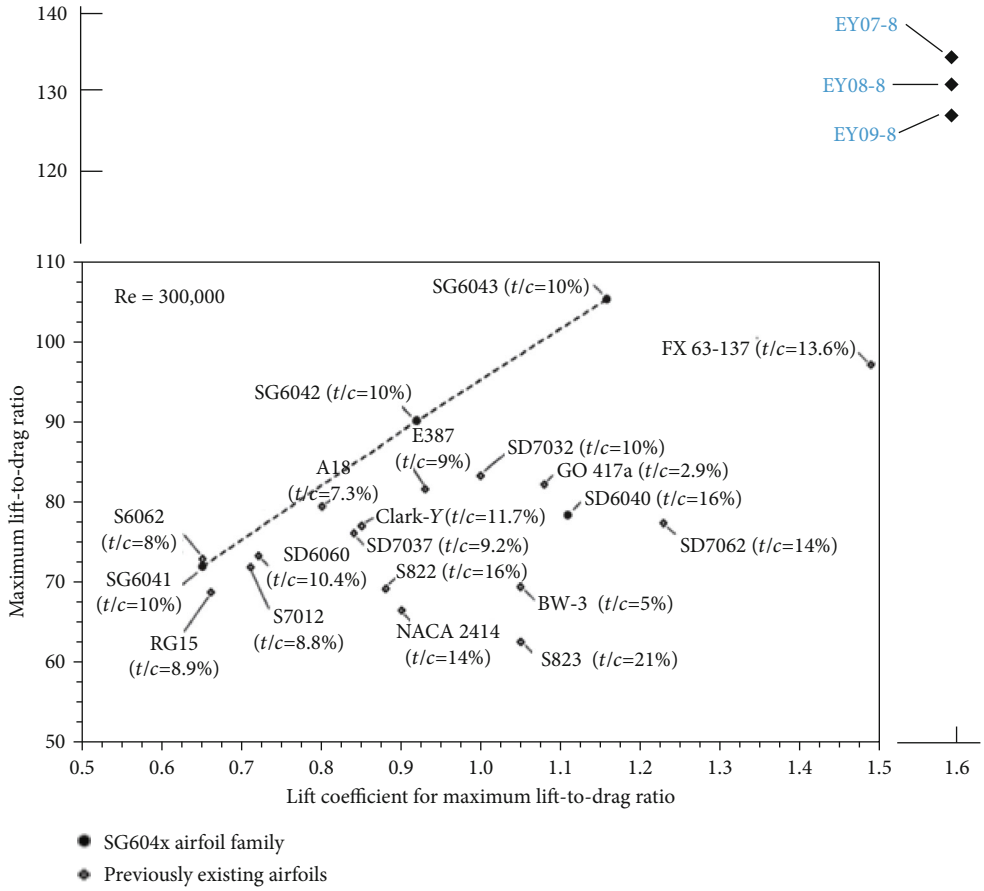


Figure 8: Airfoil performance comparisons [28].

Table 2: Airfoil performance summary.

| Author | Study conducted |
|---|---|
| Singh et al., 2012 [16] | AF300 airfoil was developed for low Re wind turbine application. Maximum $L/D$ and stall angle of 54 and 14°, respectively, were obtained at Re = 100,000. |
| Selig and McGranahan, 2004 [15] | FX63-137 airfoil was tested for low Re performance at Re = 500,000. Maximum $L/D$ and stall angle obtained were 108 and 12°, respectively. |
| Henriques et al., 2009 [30] | T.Urban 10/193 airfoil was developed for low Re wind turbine application and tested at Re = 500,000. Maximum $L/D$ and stall angle obtained were 95 and 12°, respectively. |
| Limin et al., 2011 [47] | The seagull airfoil was developed for small wind turbine application and tested at Re = 100,000, 350,000, and 600,000. Maximum $L/D$ obtained were 38, 52, and 57, respectively. |
| Shah et al., 2014 [27] | UBD6166 airfoil was developed for small wind turbine application and tested at Re = 100,000. Maximum $L/D$ of 66.9 was obtained. |
| Wata et al., 2011 [17] | SG6043_Eppler 442 airfoil was developed for small wind turbine application and tested at Re = 205,000. Maximum $L/D$ obtained was 80. |

of the base airfoil and EYO-Series airfoils at Re = 300,000 is presented in Figure 6.

From the results of Figure 6, the EYO-Series airfoils have relatively better $L/D$ performance than the SG6043 airfoil, especially for angles of attack between 0° and 9°. EYO7-8 airfoil had the highest maximum $L/D$ of 134 while SG6043 had the lowest value of 117. EYO8-8 and EYO9-8 also had maximum $L/D$ values of 131 and 127, respectively. The maximum $L/D$ for all four airfoils occurred at 5° angle of attack.

*3.3. Comparative Drag Buckets of EYO-Series Airfoils and SG6043 Base Airfoil.* The drag buckets of the SG6043 and EYO-Series airfoils at Re = 300,000 are presented in Figure 7. In airfoil design, the drag bucket gives a graphical indication of how the drag coefficient extends over a range of lift coefficients.

From Figure 7, the EYO-Series airfoils had better performing drag buckets than the SG6043 airfoil. Although the initial increases in lift occurred steadily with no corresponding

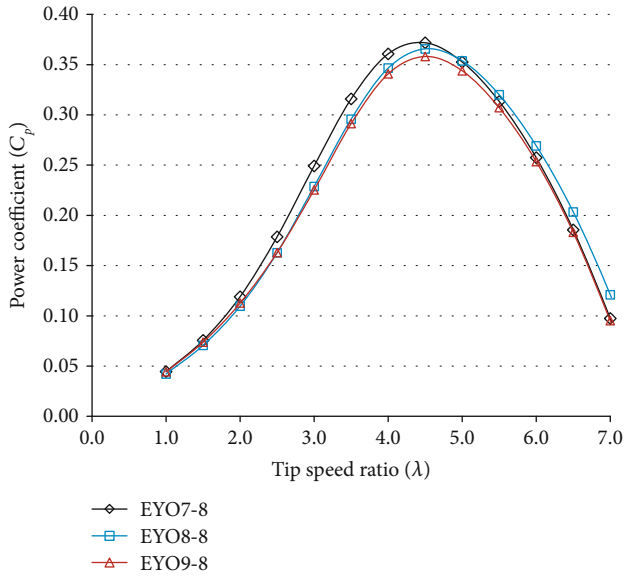


Figure 9: Power coefficient curve for wind turbine rotor.

increases in drag for all four airfoils, the drag on the SG6043 airfoil started increasing sharply above the lift coefficient of 1.4. However, the drag on the EYO-Series airfoils only started increasing at a relatively higher lift coefficient of about 1.7. Among the EYO-Series airfoils, the performance differences mainly occur beyond the drag coefficient of 0.05, where EYO9-8 has the best drag bucket performance, followed by EYO8-8 and EYO7-8.

*3.4. Airfoil Performance Summary.* To ascertain the performance of the EYO-Series airfoils in comparison with other airfoils developed by different researchers for low Re and small wind turbine applications, the $L/D$ at Re = 300,000 are presented in Figure 8 which is adapted from a study by Gigueŕe and Selig [28].

From the comparative results of Figure 8, the EYO-Series airfoils outperform the SG604x airfoil family and the others by relatively higher $L/D$ performances which occur at a relatively higher lift coefficient of about 1.6. Again, the EYO-Series airfoils, with their high lift-to-drag ratios, outperform other developed low Re airfoils presented in Table 2. These performance improvements of the new airfoils are due to the optimal $t/c$ employed in their design. The zone for the $t/c$ between 0.85 and 1.50 leads to the development of relatively thin and cambered designs which are generally known as features that improve airfoil aerodynamic performance [23, 45, 46].

*3.5. Power Generation Potential.* To be able to estimate the potential power generation from the performance characteristics of the newly developed EYO-Series airfoil designs, power coefficient curves were computed for 3-bladed 6 m diameter rotors made from each airfoil and are presented in Figure 9. The power coefficient for all three rotors had similar dome-shaped relationship with tip-speed ratio. The maximum power coefficient for all three rotors occurred at about the same tip-speed ratio of 4.5. However, the EYO7-8 rotor had the highest maximum power coefficient of 0.371, while the EYO9-8 rotor had the lowest maximum power coefficient of 0.358. The EYO8-8 rotor had maximum power coefficient of 0.366. Based on typical average wind speed in Ghana of 6.1 m/s reported by the Ghana Energy Commission, the estimated power production from the EYO7-8, EYO8-8, and EYO9-8 rotors according to Equation (11) is 1488 W, 1468 W, and 1435 W, respectively. This potential power generation from the small wind turbines meets the power demand of most residential facilities in developing countries as reported in the works of [48–51].

## 4. Conclusions

In the present study, three new airfoils (EYO-Series) for small wind turbine applications were designed and tested in XFOIL for aerodynamic performance at Re = 300,000. The airfoils were subsequently used to develop and test 3-bladed 6 m diameter wind turbine rotors for power generation. From the results, the following key findings were made:

(i) EYO7-8, EYO8-8, and EYO9-8 airfoils had maximum lift-to-drag ratios of 134, 131, and 127, respectively, and maximum lift coefficients of 1.77, 1.81, and 1.81, respectively

(ii) EYO9-8 had the highest stall angle of 15° while EYO8-8 and EYO7-8 had stall angles of 14° and 12°, respectively

(iii) The improved performance of the EYO-Series airfoils is due to the optimal $t/c$ range of 0.85 to 1.50 used for the design

(iv) Together, the EYO-Series airfoils are suitable for the design and development of small wind turbine blades

(v) Wind turbine rotor analysis also showed that the EYO7-8, EYO8-8, and EYO9-8 rotors had maximum power coefficients of 0.371, 0.366, and 0.358, respectively

## Abbreviations

$a$: Axial induction factor
$a'$: Angular induction factor
$\alpha$: Angle of attack
$\rho$: Air density
$c$: Airfoil chord
$\mu$: Dynamic viscosity
$\nu$: Kinematic viscosity
$\Omega$: Angular velocity
$\phi$: Relative airflow angle
$\theta_p$: Pitch angle
$\sigma_r$: Chord solidity
$\lambda$: Tip-speed ratio
$\lambda_r$: Local speed ratio
$\lambda_h$: Blade root speed ratio
$A$: Rotor cross-sectional area

$B$: Number of rotor blades
$C_d$: Drag coefficient
$C_L$: Lift coefficient
$C_p$: Power coefficient
$D$: Drag force
$l$: Airfoil span
$L$: Lift force
$L/D$: Lift-to-drag ratio
m: Metre
$P$: Rotor power
$r$: Radial airfoil location
Re: Reynolds number
$t/c$: Thickness to camber ratio
$U$: Free stream airflow speed
$U_{rel}$: Relative airflow speed
% c: Percentage of chord.

## Data Availability

The data used to support the findings of this study are available from the corresponding author upon request.

## Additional Points

*Further Studies*. The present study has analysed the performance of newly developed airfoil designs based on an optimal thickness-to-camber ratio ($t/c$) of 0.85–1.5, for low Reynolds number applications, using XFOIL. The results have shown that better performance of the airfoil is obtained within this optimal $t/c$ range. Future work of constructing prototypes of the airfoil designs based on the optimal $t/c$ and testing them in a wind tunnel is worth investigating.

## Conflicts of Interest

The authors declare that there is no conflict of interest regarding the publication of this paper.

## Acknowledgments

The authors acknowledge the research support by the Kwame Nkrumah University of Science and Technology (KNUST) Ghana and Norwegian University of Life Sciences (NMBU) Norway collaborative project titled "Upgrading Education and Research Capacity in Renewable Energy Technologies (UPERCRETs)," which is funded through the Energy and Petroleum (EnPe) Project of the Norwegian Agency for Development Cooperation (Norad).

## References

[1] K. Uddin, G. Prinsloo, J. Marco, and P. Jennings, "Techno-economic analysis of the viability of solar home systems using lithium-ion batteries in sub-Saharan Africa," *Energy Procedia*, vol. 138, pp. 267–272, 2017.

[2] A. A. Mas'ud, A. V. Wirba, F. Muhammad-Sukki et al., "A review on the recent progress made on solar photovoltaic in selected countries of sub-Saharan Africa," *Renewable and Sustainable Energy Reviews*, vol. 62, pp. 441–452, 2016.

[3] B. Pillot, M. Muselli, P. Poggi, and J. B. Dias, "Historical trends in global energy policy and renewable power system issues in sub-Saharan Africa: the case of solar PV," *Energy Policy*, vol. 127, pp. 113–124, 2019.

[4] J. Khan and M. H. Arsalan, "Solar power technologies for sustainable electricity generation - a review," *Renewable and Sustainable Energy Reviews*, vol. 55, pp. 414–425, 2016.

[5] T. S. Amjath-Babu, T. J. Krupnik, S. Aravindakshan, M. Arshad, and H. Kaechele, "Climate change and indicators of probable shifts in the consumption portfolios of dryland farmers in sub-Saharan Africa: implications for policy," *Ecological Indicators*, vol. 67, pp. 830–838, 2016.

[6] Y. Cai, R. Riezman, and J. Whalley, "International trade and the negotiability of global climate change agreements," *Economic Modelling*, vol. 33, pp. 421–427, 2013.

[7] Y. Gao, X. Gao, and X. Zhang, "The 2 °C global temperature target and the evolution of the long-term goal of addressing climate change–from the United Nations framework convention on climate change to the Paris agreement," *Engineering*, vol. 3, no. 2, pp. 272–278, 2017.

[8] A. A. Prasad, R. A. Taylor, and M. Kay, "Assessment of solar and wind resource synergy in Australia," *Applied Energy*, vol. 190, pp. 354–367, 2017.

[9] R. A. Rosen and E. Guenther, "The energy policy relevance of the 2014 IPCC working group III report on the macroeconomics of mitigating climate change," *Energy Policy*, vol. 93, pp. 330–334, 2016.

[10] J. A. Tambo, "Adaptation and resilience to climate change and variability in north-east Ghana," *International Journal of Disaster Risk Reduction*, vol. 17, pp. 85–94, 2016.

[11] C. Fant, B. Gunturu, and A. Schlosser, "Characterizing wind power resource reliability in Southern Africa," *Applied Energy*, vol. 161, pp. 565–573, 2016.

[12] Y. Kumar, J. Ringenberg, S. S. Depuru et al., "Wind energy: trends and enabling technologies," *Renewable and Sustainable Energy Reviews*, vol. 53, pp. 209–224, 2016.

[13] H. S. Ramadan, "Wind energy farm sizing and resource assessment for optimal energy yield in Sinai Peninsula, Egypt," *Journal of Cleaner Production*, vol. 161, pp. 1283–1293, 2017.

[14] A. F. P. Ribeiro, A. M. Awruch, and H. M. Gomes, "An airfoil optimization technique for wind turbines," *Applied Mathematical Modelling*, vol. 36, no. 10, pp. 4898–4907, 2012.

[15] M. S. Selig and B. D. McGranahan, "Wind tunnel aerodynamic tests of six airfoils for use on small wind turbines," *Journal of Solar Energy Engineering*, vol. 126, no. 4, pp. 986–1001, 2004.

[16] R. K. Singh, M. R. Ahmed, M. A. Zullah, and Y. H. Lee, "Design of a low Reynolds number airfoil for small horizontal axis wind turbines," *Renewable Energy*, vol. 42, pp. 66–76, 2012.

[17] J. Wata, M. Faizal, B. Talu, L. Vanawalu, P. Sotia, and M. R. Ahmed, "Studies on a low Reynolds number airfoil for small wind turbine applications," *SCIENCE CHINA Technological Sciences*, vol. 54, no. 7, pp. 1684–1688, 2011.

[18] S. Rehman, M. M. Alam, L. M. Alhems, and M. M. Rafique, "Horizontal axis wind turbine blade design methodologies for efficiency enhancement—a review," *Energies*, vol. 11, no. 3, p. 506, 2018.

[19] R. K. Singh and M. R. Ahmed, "Blade design and performance testing of a small wind turbine rotor for low wind speed applications," *Renewable Energy*, vol. 50, pp. 812–819, 2013.

[20] X. Tang, X. Huang, R. Peng, and X. Liu, "A direct approach of design optimization for small horizontal axis wind turbine blades," *Procedia CIRP*, vol. 36, pp. 12–16, 2015.

[21] A. Tummala, R. K. Velamati, D. K. Sinha, V. Indraja, and V. H. Krishna, "A review on small scale wind turbines," *Renewable and Sustainable Energy Reviews*, vol. 56, pp. 1351–1371, 2016.

[22] S. N. Akour, M. Al-Heymari, T. Ahmed, and K. A. Khalil, "Experimental and theoretical investigation of micro wind turbine for low wind speed regions," *Renewable Energy*, vol. 116, pp. 215–223, 2018.

[23] N. Karthikeyan, K. Kalidasa Murugavel, S. Arun Kumar, and S. Rajakumar, "Review of aerodynamic developments on small horizontal axis wind turbine blade," *Renewable and Sustainable Energy Reviews*, vol. 42, pp. 801–822, 2015.

[24] A. Chehouri, R. Younes, A. Ilinca, and J. Perron, "Review of performance optimization techniques applied to wind turbines," *Applied Energy*, vol. 142, pp. 361–388, 2015.

[25] Y. P. Ju and C. H. Zhang, "Multi-point robust design optimization of wind turbine airfoil under geometric uncertainty," *Proceedings of the Institution of Mechanical Engineers, Part A: Journal of Power and Energy*, vol. 226, no. 2, pp. 245–261, 2011.

[26] S. Rajakumar and D. Ravindran, "Iterative approach for optimising coefficient of power, coefficient of lift and drag of wind turbine rotor," *Renewable Energy*, vol. 38, no. 1, pp. 83–93, 2012.

[27] H. Shah, S. Mathew, and C. M. Lim, "A novel low Reynolds number airfoil design for small horizontal axis wind turbines," *Wind Engineering*, vol. 38, no. 4, pp. 377–391, 2014.

[28] P. Giguere and M. S. Selig, "New airfoils for small horizontal axis wind turbines," *Journal of Solar Energy Engineering*, vol. 120, no. 2, pp. 108–114, 1998.

[29] P. Giguere and M. S. Selig, "Low Reynolds number airfoils for small horizontal axis wind turbines," *Wind Engineering*, vol. 21, no. 6, pp. 367–380, 1997.

[30] J. C. C. Henriques, F. Marques da Silva, A. I. Estanqueiro, and L. M. C. Gato, "Design of a new urban wind turbine airfoil using a pressure-load inverse method," *Renewable Energy*, vol. 34, no. 12, pp. 2728–2734, 2009.

[31] G. Fernandez, H. Usabiaga, and D. Vandepitte, "An efficient procedure for the calculation of the stress distribution in a wind turbine blade under aerodynamic loads," *Journal of Wind Engineering and Industrial Aerodynamics*, vol. 172, pp. 42–54, 2018.

[32] M.-H. Lee, Y. C. Shiah, and C.-J. Bai, "Experiments and numerical simulations of the rotor-blade performance for a small-scale horizontal axis wind turbine," *Journal of Wind Engineering and Industrial Aerodynamics*, vol. 149, pp. 17–29, 2016.

[33] Q. Song and W. D. Lubitz, "Design and testing of a new small wind turbine blade," *Journal of Solar Energy Engineering*, vol. 136, no. 3, p. 4, 2014.

[34] F. O. Akuffo, A. Brew-Hammond, J. Antonio et al., *Solar and Wind Energy Resource Assessment (SWERA)*, Energy Commission, Ghana, 2003.

[35] C.-J. Bai, W.-C. Wang, P.-W. Chen, and W.-T. Chong, "System integration of the horizontal-axis wind turbine: the design of turbine blades with an axial-flux permanent magnet generator," *Energies*, vol. 7, no. 11, pp. 7773–7793, 2014.

[36] H. Hirahara, M. Z. Hossain, M. Kawahashi, and Y. Nonomura, "Testing basic performance of a very small wind turbine designed for multi-purposes," *Renewable Energy*, vol. 30, no. 8, pp. 1279–1297, 2005.

[37] F.-B. Hsiao, C.-J. Bai, and W.-T. Chong, "The performance test of three different horizontal axis wind turbine (HAWT) blade shapes using experimental and numerical methods," *Energies*, vol. 6, no. 6, pp. 2784–2803, 2013.

[38] P. J. Schubel and R. J. Crossley, "Wind turbine blade design," *Energies*, vol. 5, no. 9, pp. 3425–3449, 2012.

[39] I. Bayati, M. Belloli, L. Bernini, and A. Zasso, "Aerodynamic design methodology for wind tunnel tests of wind turbine rotors," *Journal of Wind Engineering and Industrial Aerodynamics*, vol. 167, pp. 217–227, 2017.

[40] J. F. Manwell, J. G. Mcgowan, and A. L. Rogers, *Wind Energy Explained: Theory, Design and Application. Second Edition*, John Wiley & Sons Ltd, 2009.

[41] A. Hassanzadeh, A. Hassanzadeh Hassanabad, and A. Dadvand, "Aerodynamic shape optimization and analysis of small wind turbine blades employing the Viterna approach for post-stall region," *Alexandria Engineering Journal*, vol. 55, no. 3, pp. 2035–2043, 2016.

[42] J. Martinez, L. Bernabini, O. Probst, and C. Rodriguez, "An improved BEM model for the power curve prediction of stall-regulated wind turbines," *Wind Energy*, vol. 8, no. 4, pp. 385–402, 2005.

[43] M. Refan and H. Hangan, "Aerodynamic performance of a small horizontal axis wind turbine," *Journal of Solar Energy Engineering*, vol. 134, no. 2, pp. 1–7, 2012.

[44] T. Burton, N. Jenkins, D. Sharpe, and E. Bossanyi, *Wind Energy Handbook, Second Edition*, John Wiley & Sons Ltd, 2011.

[45] P. Giguere and M. S. Selig, "Aerodynamic effects of leading-edge tape on aerofoils at low Reynolds numbers," *Wind Energy*, vol. 2, no. 3, pp. 125–136, 1999.

[46] T. Göçmen and B. Özerdem, "Airfoil optimization for noise emission problem and aerodynamic performance criterion on small scale wind turbines," *Energy*, vol. 46, no. 1, pp. 62–71, 2012.

[47] Q. Limin, S. Wei, R. Gu, X. Quan, and Y. Yang, "The investigation of the airfoil for the small wind turbine based on the seagull airfoil," in *2011 Asia-Pacific Power and Energy Engineering Conference*, pp. 1–4, Wuhan, China, March 2011.

[48] Y. Abdul-salam and E. Phimister, "The politico-economics of electricity planning in developing countries: a case study of Ghana," *Energy Policy*, vol. 88, pp. 299–309, 2016.

[49] W. Athukorala, C. Wilson, S. Managi, and M. Karunarathna, "Household demand for electricity: the role of market distortions and prices in competition policy," *Energy Policy*, vol. 134, article 110932, 2019.

[50] N. S. Ouedraogo, "Modeling sustainable long-term electricity supply-demand in Africa," *Applied Energy*, vol. 190, pp. 1047–1067, 2017.

[51] Y. Ye, S. F. Koch, and J. Zhang, "Determinants of household electricity consumption in South Africa," *Energy Economics*, vol. 75, pp. 120–133, 2018.